Desalination and Water Treatment
www.deswater.com
doi: 10.1080/19443994.2015.1032359

57 (2016) 9837–9844
May

Taylor & Francis
Taylor & Francis Group

Preparation of Zn-TiO_2/RH/Fe_3O_4 composite material and its photocatalytic degradation for the dyes in wastewater

Yili Ge*, Ying Xiang, Yu He, Meiyan Ji, Gongwu Song*

Ministry-of-Education Key Laboratory for the Synthesis and Application of Organic Functional Molecules, Hubei Collaborative Innovation Center for Advanced Organic Chemical Materials, Hubei University, Wuhan, China, Tel. +86 27 88662747; emails: geyili2007@aliyun.com (Y. Ge), beatasmile@hotmail.com (Y. Xiang), 43160562@qq.com (Y. He), 316728369@qq.com (M. Ji), songgw@hubu.edu.cn (G. Song)

Received 31 July 2014; Accepted 17 March 2015

ABSTRACT

A versatile Zn-TiO_2/RH/Fe_3O_4 ternary composite material on the basis of rice hull was prepared and characterized by X-ray diffraction, Fourier transform infrared spectroscopy (FT-IR), scanning electron microscopy, energy dispersive X-ray spectroscopy, and vibrating sample magnetometer analysis. Its ability to photocatalytically remove Rhodamine B (RhB) in wastewater was investigated in a photochemical reactor by means of ultraviolet and visible spectrophotometry and FT-IR. Research results show that the catalytic degradation rate of RhB from aqueous solution is close to 100% when using synthesized Zn-TiO_2/RH/Fe_3O_4 as a catalyst under irradiation of visible light for 120 min. The as-prepared visible light-driven photocatalyst Zn-TiO_2/RH/Fe_3O_4 material has high performance with excellent recyclability, magnetic separation feature, and photocatalysis activity in wastewater treatment.

Keywords: Rice hull (RH); Composite material; Rhodamine B (RhB); Photocatalyst; Degradation

1. Introduction

Dyes that have complex organic components and non-biodegradable structures can cause carcinogenic and mutagenic effects and make water bodies unsuitable for human use [1]. Consequently, dyes in surface and groundwater cause important environmental concerns and need to be removed [2]. To date, numerous adsorbents have been used to remove dyes [3]. However, most of them are hazardous chemicals and/or need harsh reaction conditions for their degradation [4]. Adsorbents based on rice hull or rice husk (RH), an abundant agricultural by-product and waste, have the advantages of ecological friendliness and origin from a broad source of raw materials. Typically, RH consists of ~75% organic substances (cellulose, lignin, and hemicelluloses), 15% amorphous SiO_2 and 10% water and microelements [5]. However, the application of naturally available RH-based adsorbents only achieves a low removal rate of dyes. Therefore, there is a critical need to develop inexpensive modified RH adsorbents with efficient adsorption and degradation of dyes. Surface functionalization technology has been proved to be very effective in enhancing RH function [6,7]. TiO_2 is an excellent photocatalyst because of its high photocatalytic efficiency, low-cost and

*Corresponding authors.

nontoxicity. It is often used to remove organic pollutants from wastewater in the past decades. However, TiO_2 is only responsive to UV irradiation due to its wide bandgap and the lack of TiO_2 photocatalytic activity with visible light restricts its application in environmental treatment [8]. The method of doping TiO_2 with transition metals (such as Zn) having electronic coupling capability can be used to promote photocatalytic activity of TiO_2 under visible light [9]. Magnetic photocatalysts are promising materials for overcoming the drawbacks of photocatalyst separation and recovery [10]. Although many investigations have been carried out concerning the doping of a semiconductor surface with metal ions, little work has been reported concerning doping in magnetic TiO_2 [11]. Therefore, the present study focuses on the efficient utilization of visible light and the abilities in photocatalytic activity and the recyclability of photocatalyst materials. In the present research, a novel Zn-TiO_2/RH/Fe_3O_4 ternary magnetically separable composite material was explored and prepared. The photocatalytic activity and degradation mechanism of the as-prepared material for the photodegradation of Rhodamine B (RhB, a synthesized dye), which exhibits high stability under various conditions with considerably high resistance to photo and oxidative degradation [12], from wastewater were investigated.

2. Experimental

2.1. Materials

RhB and polyethyleneimine (PEI) were purchased from Aladdin Industrial Corporation. RH and TiO_2 sols were obtained from Wuhan University of Science and Technology. $FeCl_3{\cdot}6H_2O$ was bought from Tianjing Tianli Chemical Corporation. All the other chemicals were of analytical grade.

2.2. Preparation of Zn-TiO_2/RH/Fe_3O_4

For the synthesis of Zn-TiO_2/RH, RH was pretreated with diluted HCl solution and dried in an oven. Following this step, the pretreated RH was impregnated in $ZnCl_2$ solution for 12 h, dipped in TiO_2 sol for 24 h, and dried in an oven. The resulting materials were then protected with nitrogen at 550℃ for 3 h and cooled to room temperature to obtain Zn-TiO_2/RH. The preparation of Fe_3O_4 magnetic nanoparticles was performed according to the literature method [13]. First, 1.35 g of $FeCl_3$ was added to 35 mL of ethylene glycol and treated with ultrasonic oscillations. Then, 3.6 g of NaAc and 1.1 g of PEI were added and stirred for 30 min at room temperature. Finally, the mixed solution was placed in a reaction kettle with 50 mL of polyethylene liner at 200℃ for 10 h, washed with alcohol and water, respectively, and dried in an oven at 80℃; 0.15 g of Fe_3O_4 magnetic nanoparticle was added to 50 mL of ethylene glycol and treated with ultrasonic irradiation to form Fe_3O_4 dispersion. To prepare Zn-TiO_2/RH/Fe_3O_4, 3 g of Zn-TiO_2/RH was added to Fe_3O_4 dispersion. The resulting mixture was then shaken in a gyrotron oscillator for 4 h and dried in an oven.

2.3. Characterization of Zn-TiO_2/RH/Fe_3O_4 composite material

In order to analyze the morphology of Zn-TiO_2/RH/Fe_3O_4, X-ray diffraction (XRD) analysis was carried out using D/MAX-IIIC X-ray diffractometer (Rigaku Corporation, Japan). The X-ray source was Cu Kα radiation (λ = 0.15406 nm) with working current (40 mA) and voltage (40 kV). The morphology of Zn-TiO_2/RH/ Fe_3O_4 was also analyzed using high-resolution images obtained with a JEOL (Japan) JSM6510LV scanning electron microscope coupled with energy dispersive X-ray spectrometer (SEM/EDX). The magnetic behavior of the composite material was investigated by HH-15 vibrating sample magnetometer (VSM, China). The UV–Vis and Fourier transform infrared (FT-IR) spectra of RhB before and after degradation were analyzed using Perkin-Elmer Lambda 35 and Perkin-Elmer Spectrum one FT-IR (USA), respectively.

2.4. Photocatalytic degradation of RhB using Zn-TiO_2/RH/Fe_3O_4

The concentration of RhB (its structure as shown in Fig. 1) in aqueous solution (simulating wastewater of printing and dyeing) was determined through

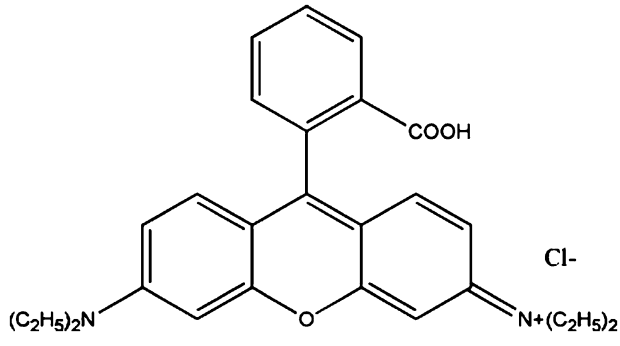

Fig. 1. Structure of RhB [14].

measuring the absorbance A_0 of the solution at a wavelength of 554 nm by UV–Vis. The photocatalytic degradation study was carried out in a photocatalytic reactor (the light source used was metal halide lamp). The composite material Zn-TiO_2/RH/Fe_3O_4 was added to the dye solution in the photocatalytic reactor and taken out every 20 min. The absorbance A of the dye supernatant solution was determined at a wavelength of 554 nm. The value of A/A_0 represents the residual quantity of RhB in wastewater and the degradation rate of RhB was calculated using the equation: $(1 - A/A_0) \times 100\%$.

3. Results and discussion

3.1. Characterization and analysis

3.1.1. XRD analysis

To determine if Zn-TiO_2/RH/Fe_3O_4 is successfully synthesized, we analyzed the XRD patterns of Fe_3O_4, Zn-TiO_2/RH and Zn-TiO_2/RH/Fe_3O_4 composite materials. In the XRD patterns, Zn-TiO_2/RH displays the diffraction peaks at 25.14°, 25.28°, 26.17°, and 54.58° (Fig. 2), indicating that the crystal phase of Zn-TiO_2 is anatase/rutile mischcrystal, since their characteristic peaks exist simultaneously in the XRD pattern. Zn exists as a dopant because there are no diffraction peaks of ZnO_2 (it decomposes at 182°C) and ZnO in the XRD pattern of the composite. Fe_3O_4 has the characteristic peaks at 35.56°, 57.08°, and 62.77° in the XRD pattern (Fig. 2). These characteristic peaks were still observed in the XRD pattern of Zn-TiO_2/RH/Fe_3O_4 (Fig. 2), demonstrating that Zn-TiO_2/RH/Fe_3O_4 is successfully synthesized.

3.1.2. FT-IR analysis

To further confirm that Zn-TiO_2/RH/Fe_3O_4 is successfully prepared, we analyzed the FT-IR spectra of Zn-TiO_2/RH and Zn-TiO_2/RH/Fe_3O_4. In the spectrum of Zn-TiO_2/RH, the peaks at 3,013, 2,919, and 2,849 cm^{-1} are assigned to $–CH_3$ and $–CH_2$ stretching and bending vibrations, respectively (Fig. 3). The band at 3,013 cm^{-1} corresponds to a three-member cycle of carbon structure. In the spectrum of Zn-TiO_2/RH/Fe_3O_4, the characteristic peak at 3,013 cm^{-1} disappears, and the peaks of 2,919 and 2,849 cm^{-1} shift to 2,976 and 2,920 cm^{-1}, respectively, accompanied by peak broadening (Fig. 3). This result indicates the open loop of a three-member cycle, the partial carbonization of $–CH_3$ and $–CH_2$, and the formation of hydrogen bond with Fe_3O_4 after the reaction. The broadening and heightening of the peak at 3,427 cm^{-1} is the marker of hydrogen bond (Fig. 3), further proving the formation of hydrogen bond with Fe_3O_4 in Zn-TiO_2/RH/Fe_3O_4 molecule. The existence of the sharp peaks at the 2,354 cm^{-1} and 2,320 cm^{-1} in the spectrum of Zn-TiO_2/RH indicates that there is the –O–C=O structure but no other O–C bond in the abutting carbon structure frame (Fig. 3). However, the above peaks broaden and weaken in intensity *in situ* in the spectrum of Zn-TiO_2/RH/Fe_3O_4 which indicates the existence of the adjacent oxygen atom derived from Fe_3O_4. Thus, Fe_3O_4 is effectively hybridized into Zn-TiO_2/RH. Compared with the spectrum of Zn-TiO_2/RH, the intensity of the peak at 1,067 cm^{-1} corresponding to the C=C–H stretching and bending vibrations increases in that of Zn-TiO_2/RH/Fe_3O_4, demonstrating that intense carbonization and dehydration reactions indeed take place in carbon frame structures (Fig. 3). Since C=C is an electron-rich system, it is readily

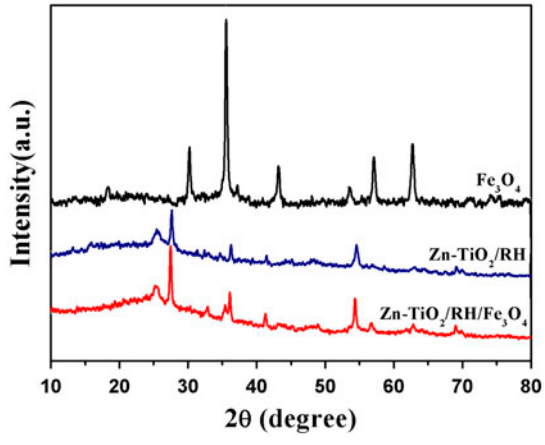

Fig. 2. XRD patterns of Zn-TiO_2/RH/Fe_3O_4 composite material.

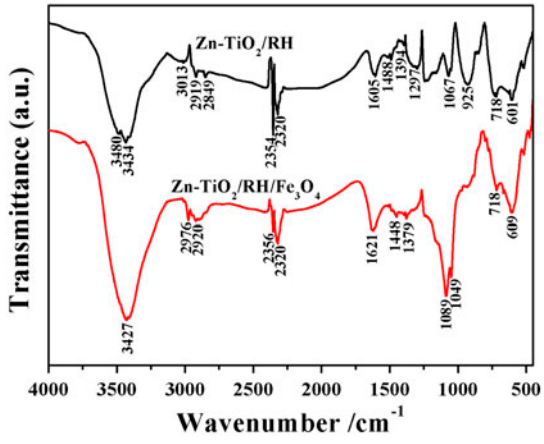

Fig. 3. FT-IR spectra of Zn-TiO_2/RH/Fe_3O_4 composite material.

coordinated to some heavy metals such as Ti, Fe, and Zn to produce an electron-rich coordination system. While Fe_3O_4 is a crystal defect matter, it easily combines with the carbon–carbon double bond of the electron-rich system. This deduction is proved by the increase in the peak height at 1,067 cm^{-1}. The peak at 1,297 cm^{-1} corresponding to the C–O stretching vibration disappears in the spectrum of Zn-TiO_2/RH/Fe_3O_4 (Fig. 3) because electron-rich oxygen atoms with unshared electron pairs are much too apt to become the electron donors for the hydrogen bond and the coordination system. According to the FT-IR spectra (Fig. 3), the coordination reaction of C=C–H and –O with Fe as well as the formation of the hydrogen bond of C–O and C=O with –H testifies that the Zn-TiO_2/RH/Fe_3O_4 composite material is successfully prepared.

3.1.3. SEM/EDX analysis

In order to determine the morphological features and elemental species of the synthesized materials in the process of preparation, these materials were characterized by SEM/EDX measurements. RH has some porous structures, and its chemical compositions consist of C, O, and Si elements (Fig. 4(a)). The SEM image in Fig. 4(b) shows that the Ti–Zn film is formed on the pore wall and surface of RH specimens after Ti–Zn sol impregnation and hot treatment, and the EDX in Fig. 4(b) reveals the presence of Ti and Zn elements in Zn-TiO_2/RH. The SEM/EDX results of Zn-TiO_2/RH/Fe_3O_4 (Fig. 4(c)) reveal that the Fe_3O_4 magnetosphere is attached to the Zn-TiO_2/RH composite material and the EDX spectrum validates the presence of element Fe in the as-prepared Zn-TiO_2/RH/Fe_3O_4 (Fig. 4).

3.1.4. Magnetic property analysis

Next, we determined the magnetic properties of the Zn-TiO_2/RH/Fe_3O_4 composite by means of VSM. The saturation magnetization of the composite material is 0.63 emu g^{-1} according to the hysteresis loops in Fig. 5(a) and the schematic diagram of Fig. 5(b) shows that the Zn-TiO_2/RH/Fe_3O_4 composite material can be attracted by a magnet. The testing result indicates that the prepared material can be quickly separated from the treated wastewater solution in the presence of an external magnetic field. Thus, the magnetic load on the Zn-TiO_2/RH/Fe_3O_4 material is beneficial to its magnetic separation and recycling of the photocatalyst in wastewater treatment.

3.2. Degradation tests of RhB

3.2.1. Effect of pH on RhB degradation

We next asked if the Zn-TiO_2/RH/Fe_3O_4 composite material can efficiently degrade RhB under

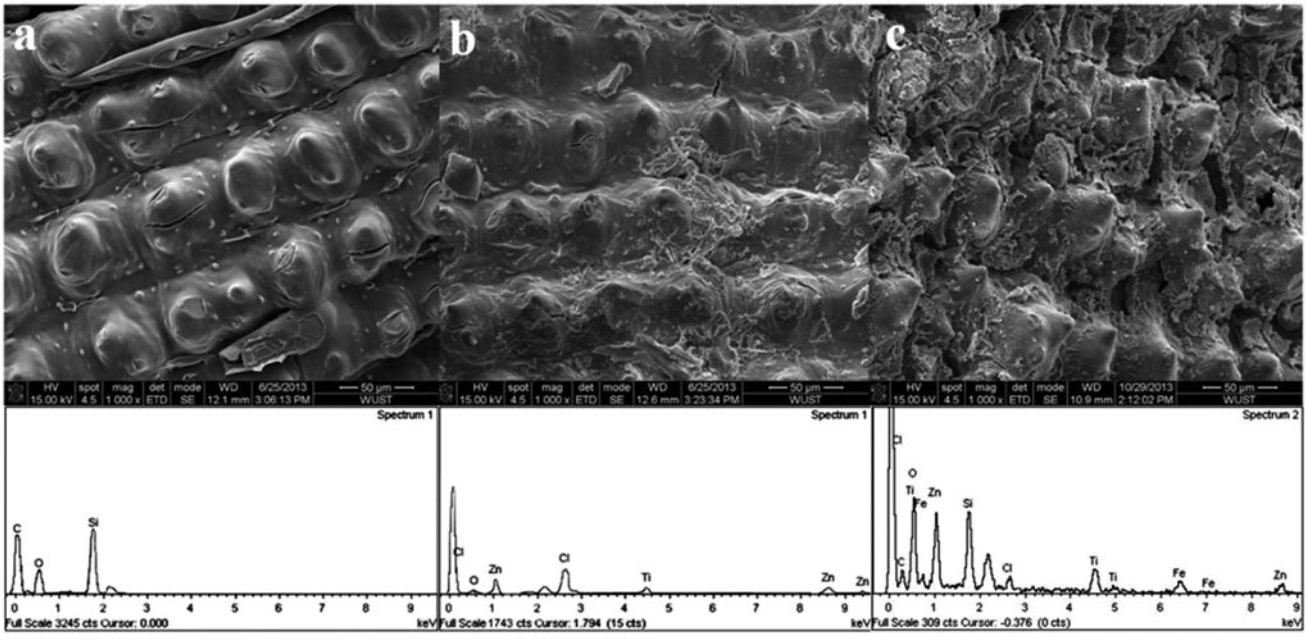

Fig. 4. SEM images and EDX spectra of rice husk (a), Zn-TiO_2/RH (b), and Zn-TiO_2/RH/Fe_3O_4 (c).

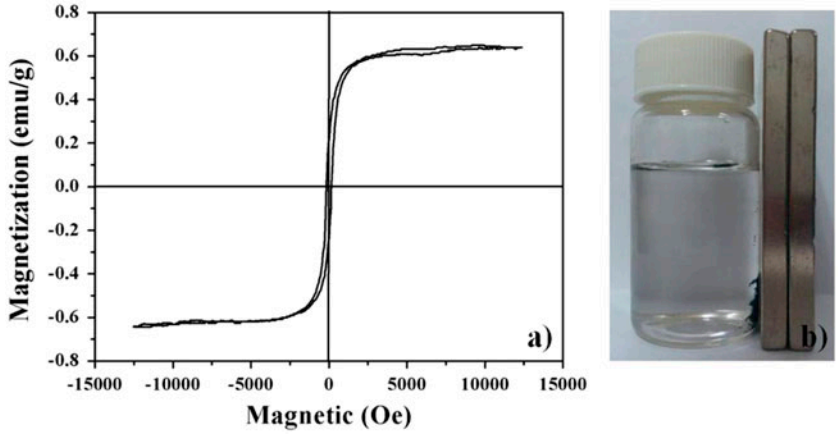

Fig. 5. Hysteresis loops of Zn-TiO_2/RH/Fe_3O_4 composite material (a) and schematic diagram of the magnetic separation of Zn-TiO_2/RH/Fe_3O_4 from aqueous solution (b).

various pH conditions. To test this, initial concentrations of RhB were set at 2.00×10^{-5} mol L^{-1} in 25 mL of aqueous solutions in quartz tubes, and the initial pH of the solution was adjusted with H_2SO_4 and NaOH solutions to 2.5, 4.0, 6.3, and 10.5, respectively; 1.00 g L^{-1} Zn-TiO_2/RH/Fe_3O_4 composite material was added to the solutions in the quartz tubes. The photocatalytic degradation experiment was carried out after the adsorption equilibrium of RhB on the surface of the Zn-TiO_2/RH/Fe_3O_4 composite had been established without irradiation of visible light. The tubes were then placed into a photochemical reactor to start the reaction. The supernatants in the tubes were taken out every 20 min to determine their absorbances. The A/A_0 value of RhB changes a little as the pH value of the solution is increased from 2.5 to 10 with the same degradation time (Fig. 6), suggesting that the pH of the solution has little effect on the degradation rate of RhB. The value of A/A_0 reaches approximately zero after 120 min of visible light irradiation under all of the above pH conditions. This result shows that the photocatalytic degradation rate of RhB in aqueous solution is close to 100% in the presence of the Zn-TiO_2/RH/Fe_3O_4 photocatalyst after 2 h. Therefore, the Zn-TiO_2/RH/Fe_3O_4 composite material used in the adsorption and photocatalysis degradation of RhB under visible light irradiation is very effective in actual application.

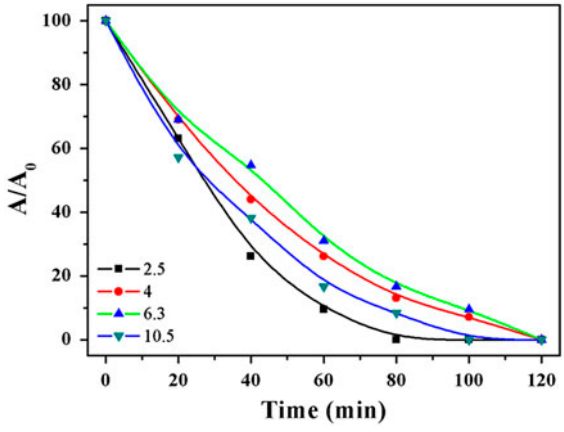

Fig. 6. Effects of initial pH on RhB degradation of RhB 2.00×10^{-5} mol L^{-1}, catalyst 1.00 g L^{-1}, and pH 2.5, 4.0, 6.3, and 10.5.

3.2.2. Effects of different materials on dye degradation

The RhB photocatalytic degradation experiments were carried out in 25 mL of RhB aqueous solution at an initial concentration of 2.00×10^{-5} mol L^{-1} in four quartz tubes. Moreover, 1.00 g L^{-1} Fe_3O_4, Zn-TiO_2/RH, and Zn-TiO_2/RH/Fe_3O_4 composite material were added to the three quartz tubes as photocatalysts, respectively. No photocatalyst was added to one of the quartz tubes as a blank control. All the quartz tubes were placed into a photochemical reactor to start the reaction. The supernatants in the tubes were taken out at a 20 min interval to determine the absorbances. As shown in Fig. 7, the removal processes of RhB in the presence of Fe_3O_4 and in the blank control follow similar invariable trends within 120 min, revealing that the degradation actions of visible light on RhB can be ignored in both the absence and presence of the Fe_3O_4 photocatalyst. In contrast, both Zn-TiO_2/RH and Zn-TiO_2/RH/Fe_3O_4 display the ability to degrade RhB, although the activity of Zn-TiO_2/RH/Fe_3O_4 for RhB degradation is slightly weaker than that of

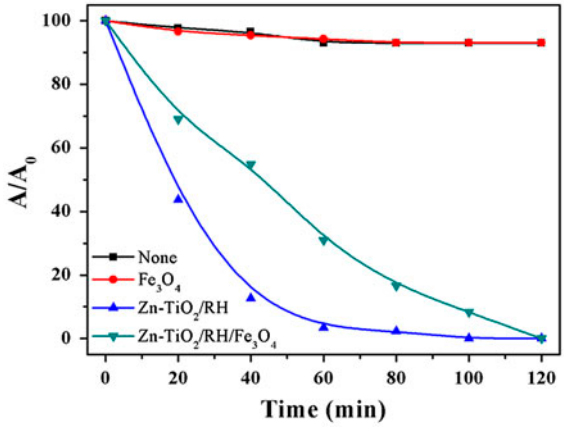

Fig. 7. RhB removal efficiencies using different catalysis degradation materials.
RhB: 2.00×10^{-5} mol L^{-1}, catalyst: 1.00 g L^{-1}.

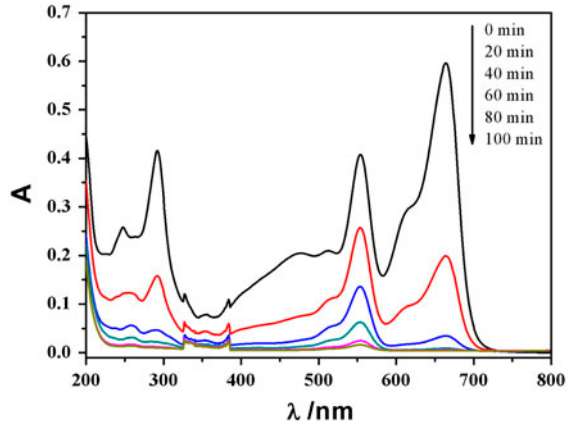

Fig. 8. Photodegradation of mixed dye by Zn-TiO_2/RH/Fe_3O_4 material.
RhB, MB, and MO are 8.00×10^{-6} mol L^{-1}, respectively, and catalyst is 1.00 g L^{-1}.

Zn-TiO_2/RH (Fig. 7). Since Zn-TiO_2/RH/Fe_3O_4 can be separated using magnetic field after degradation reaction, this result demonstrates that Zn-TiO_2/RH/Fe_3O_4 is an excellent photocatalytic material with recycle potential.

3.2.3. Degradation of mixed dyes

In order to investigate the photocatalytic activity of Zn-TiO_2/RH/Fe_3O_4 for degradation of dyes, the initial concentrations of RhB, MB (methylene blue), and MO (methyl orange) were set at 8.00×10^{-6} mol L^{-1}, respectively, in 25 mL of mixed dyes solutions in quartz tubes; 1.00 g L^{-1} of Zn-TiO_2/RH/Fe_3O_4 photocatalyst was added to each tube. Quartz tubes were placed in a photochemical reactor and the supernatants in the tubes were fetched out every 20 min to determine the absorbances. The dependences of dye photodegradation on irradiation time under visible light are revealed in Fig. 8. The maximum absorption peaks of MB (λ_{max} = 664 nm), RhB (λ_{max} = 554 nm), and MO (λ_{max} = 463 nm) of the mixed dye solution gradually diminish to disappear following the increase in the irradiation time (Fig. 8). At the same time, the characteristic absorption peak at 259 nm corresponding to benzene ring is gradually vanished. This result demonstrates that the prepared photocatalyst Zn-TiO_2/RH/Fe_3O_4 has preferable photodegradation effects on every dye in the mixed dye solution.

3.2.4. UV–Vis spectra analysis for RhB degradation

In order to explore the mechanism for degradation of RhB, UV–Vis scan in all wave bands for the intermediates in the degradation system was used to monitor the degradation process of RhB in the presence of Zn-TiO_2/RH/Fe_3O_4 photocatalyst. The absorbances of RhB supernatant solutions exposed to visible light irradiation at different times are exhibited in Fig. 9. The absorbances of RhB solutions vary with irradiation time for all samples. The characteristic absorption peaks of RhB at 259, 353, and 554 nm corresponding to the benzene ring structure and chromophores are obvious at the first time point in Fig. 9. The absorption peak at 554 nm gradually

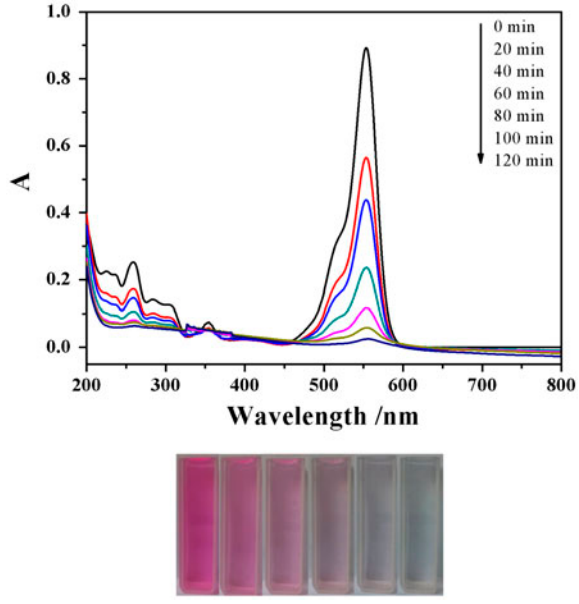

Fig. 9. Scan in all wave bands for the intermediates in the degradation system.

diminishes to disappear with the increase in the irradiation time, illustrating that the chromophores of RhB are of open loop and degraded. The absorption peak of the benzene ring at 259 nm also gradually weakens and fades away. It attests that the benzene ring is opened and this deduction can be authenticated further by FT-IR spectra.

3.2.5. FT-IR spectrum analysis before and after dye degradation

To further investigate the RhB photodegradation mechanism, FT-IR spectra of RhB before and after its adsorption degradation were analyzed. The characteristic peaks of the benzene ring are at 1,589, 1,469, and 923 cm^{-1} (Fig. 10(b)). The bands around 1,180, 1,344, and 1,274 cm^{-1} are the characteristic peaks of the C–N bond, $–CH_3$, and C–H on double bond, respectively (Fig. 10(b)).

As shown in Fig. 10(a), both the numbers and intensities of absorption peaks decrease after the photocatalytic decomposition of RhB by Zn-TiO_2/RH/Fe_3O_4 materials. The characteristic peaks of the benzene ring at 1,589 and 923 cm^{-1} as well as the characteristic peak of $–CH_3$ at 1,344 cm^{-1} disappear. These results confirm that the complex macromolecular radicals of RhB are opened up to form micromolecular compounds (such as CO_2 and water) after its degradation, demonstrating that the photocatalytic activity of Zn-TiO_2/RH/Fe_3O_4 composite material is satisfactory. The results from the above experiments disclose that the photocatalytic response of Zn-TiO_2/RH/Fe_3O_4 in the visible light region is perfect, since the bandgap of TiO_2 can be tuned by doping TiO_2 with Zn. Based on these analyses (Figs. 9 and 10), we

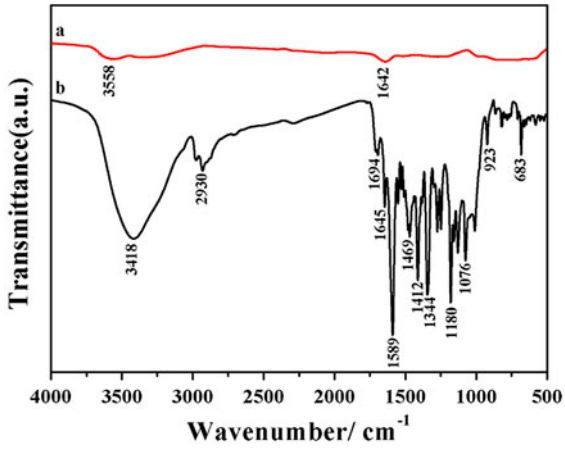

Fig. 10. FT-IR spectra before and after RhB degradation: (a) RhB after degradation; (b) RhB before degradation.

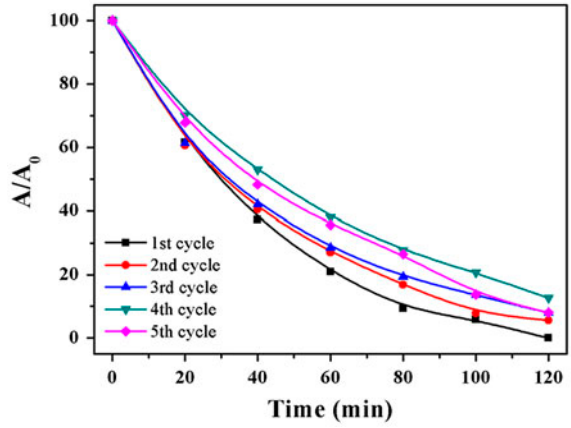

Fig. 11. Repeated utilization factor of Zn-TiO_2/RH/Fe_3O_4 photocatalyst RhB 2.00×10^{-5} mol L^{-1}, photocatalyst, 1.00 g L^{-1}.

speculate that RhB may be degraded by ·OH free radicals according to the literature report [15], which may be produced in aqueous solution by the composite material Zn-TiO_2/RH/Fe_3O_4 with visible light irradiation. However, we cannot rule out other possibilities in our photodegradation experiment. We plan to perform more experiments to verify the hypothesized photocatalytic degradation mechanism of RhB and publish the results in near future.

3.2.6. Recycling of Zn-TiO_2/RH/Fe_3O_4 composite material

We next examined recycling feasibility of Zn-TiO_2/RH/Fe_3O_4. After the Zn-TiO_2/RH/Fe_3O_4 materials were magnetically separated, recovered, and rinsed, their effects on RhB degradation were tested (as shown in Fig. 11). It shows that after recycled five times, Zn-TiO_2/RH/Fe_3O_4 has the same removal efficiency as the fresh one, demonstrating that the as-prepared Zn-TiO_2/RH/Fe_3O_4 materials have higher reutilization and reproducibility for RhB degradation. Therefore, Fe_3O_4-coated magnetic composite material facilitates the reuse of the catalyst in wastewater treatment.

4. Conclusions

In this study, the preparation of Zn-TiO_2/RH/Fe_3O_4 composite material and its photocatalytic degradation of the RhB dye in wastewater have been investigated. The analysis results of XRD, UV–Vis, FT-IR, SEM/EDX, and VSM for Zn-TiO_2/RH/Fe_3O_4 show that a ternary RH-based multifunctional

composite material is successfully synthesized. The magnetically separable characteristic of Zn-TiO_2/RH/Fe_3O_4 material provides an effective approach for recovering and reusing this photocatalyst. The UV–Vis analysis discloses that the degradation rate of RhB is nearly 100% when using visible light-driven Zn-TiO_2/RH/Fe_3O_4 as a photocatalyst for 2 h. In addition, we show that the recycling of Zn-TiO_2/RH/Fe_3O_4 has no effect on its function in degrading RhB. These results demonstrate that as a photocatalyst material, Zn-TiO_2/RH/Fe_3O_4 has higher degradation activity and preferable reutilization and can be used to solve the difficulties in the utilization of visible light, recovery, and recycling of photocatalysts in the application of wastewater treatment and environmental monitoring.

Acknowledgment

This work was supported by the National Natural Science Foundation of China under grant number 61301048 and the Foundation of Engineering Research Center of Nano-Geomaterials of the Ministry of Education under Grant No. GUGNGM201207.

References

[1] M.D.G. de Luna, E.D. Flores, D.A.D. Genuino, C.M. Futalan, M.W. Wan, Adsorption of Eriochrome Black T (EBT) dye using activated carbon prepared from waste rice hulls—Optimization, isotherm and kinetic studies, J. Taiwan Inst. Chem. Eng. 44 (2013) 646–653.

[2] Y.S. Woo, M. Rafatullah, A.F.M. Al-Karkhi, T.T. Tow, Removal of Terasil Red R dye by using Fenton oxidation: A statistical analysis, Desalin. Water Treat. 52 (2014) 4583–4591.

[3] M.T. Yagub, T.K. Sen, S. Afroze, H.M. Ang, Dye and its removal from aqueous solution by adsorption: A review, Adv. Colloid Interface Sci. 209 (2014) 172–184.

[4] P.P. Gan, S.F. Li, Efficient removal of Rhodamine B using a rice hull-based silica supported iron catalyst by Fenton-like process, Chem. Eng. J. 229 (2013) 351–363.

[5] K. Kenes, O. Yerdos, M. Zulkhair, D. Yerlan, Study on the effectiveness of thermally treated rice husks for petroleum adsorption, J. Non-Cryst. Solids 358 (2012) 2964–2969.

[6] F. Adam, J.N. Appaturi, Z. Khanam, R. Thankappan, M.A.M. Nawi, Utilization of tin and titanium incorporated rice husk silica nanocomposite as photocatalyst and adsorbent for the removal of methylene blue in aqueous medium, Appl. Surf. Sci. 264 (2013) 718–726.

[7] A.R. Khataee, M. Zarei, R. Ordikhani-Seyedlar, Heterogeneous photocatalysis of a dye solution using supported TiO_2 nanoparticles combined with homogeneous photoelectrochemical process: Molecular degradation products, J. Mol. Catal. A: Chem. 338 (2011) 84–91.

[8] Z.P. Li, Y.Q. Wen, J.P. Shang, M.X. Wu, L.F. Wang, Y. Guo, Magnetically recoverable Cu_2O/Fe_3O_4 composite photocatalysts: Fabrication and photocatalytic activity, Chin. Chem. Lett. 25 (2014) 287–291.

[9] R.R. Bhosale, S.R. Pujari, G.G. Muley, S.H. Patil, K.R. Patil, M.F. Shaikh, A.B. Gambhire, Solar photocatalytic degradation of methylene blue using doped TiO_2 nanoparticles, Sol. Energy 103 (2014) 473–479.

[10] J.J. Liu, S.L. Zuo, L.M. Yu, Y.C. Yu, B.S. Li, P.W. Chen, Visible light photodegradation of methylene blue by AgBr–$TiO_2/SiO_2@Fe_3O_4$ magnetic photocatalysts, Particuology 11 (2013) 728–731.

[11] J. Cui, T. He, X. Zhang, Synthesis of $Fe_3O_4@SiO_2@Pt_{ion}$–TiO_2 hybrid composites with high efficient UV–visible light photoactivity, Catal. Commun. 40 (2013) 66–70.

[12] X. Liu, D.J. Lee, Thermodynamic parameters for adsorption equilibrium of heavy metals and dyes from wastewaters, Bioresour. Technol. 160 (2014) 24–31. Available from: <http://dx.doi.org/10.1016/j.biortech.2013.12.053>.

[13] H. Deng, X.L. Li, Q. Peng, X. Wang, J.P. Chen, Y.D. Li, Monodisperse magnetic single-crystal ferrite microspheres, Angew. Chem. Int. Ed. 44 (2005) 2782–2785.

[14] C.K. Xu, H.H. Wu, F.L. Gu, Efficient adsorption and photocatalytic degradation of Rhodamine B under visible light irradiation over BiOBr/montmorillonite composites, J. Hazard. Mater. 275 (2014) 185–192.

[15] T.T. Tran. T, P. Sheng, C.A. Huang, J.Z. Li, L. Chen, L.J. Yuan, C.A. Grimes, Q. Cai, Synthesis and photocatalytic application of ternary Cu–Zn–S nanoparticle-sensitized TiO_2 nanotube arrays, Chem. Eng. J. 210 (2012) 425–431.